Journal of Sound and Vibration (1999) **220**(1), 1–25
Article No. jsvi.1998.1887, available online at http://www.idealibrary.com on IDEAL

FREE OUT-OF-PLANE VIBRATIONS OF A ROTATING BEAM WITH NON-LINEAR ELASTOMERIC CONSTRAINTS

G. Pohit and A. K. Mallik

Department of Mechanical Engineering, Indian Institute of Technology, Kanpur, U.P. 208016, India

and

C. Venkatesan

Department of Aerospace Engineering, Indian Institute of Technology, Kanpur, U.P. 208016, India

(*Received* 22 *August* 1997, *and in final form* 22 *July* 1998)

Free, out-of-plane vibration of a rotating beam with a non-linear, elastomeric constraint has been investigated. The elastomer is modelled as a parallel combination of spring and damper elements. The stiffness and damping parameters are evaluated by using previous experimental data. The linear analysis is performed by two techniques, one based on a power series expansion and the other based on the Rayleigh–Ritz principle. The results are found to be in excellent agreement. In the non-linear analysis, a numerical–perturbation technique is applied to determine the frequency–amplitude relationship. A parametric study revealing the influence of the non-linear constraint is presented.

1. INTRODUCTION

Dynamic analysis of rotating beams plays an important role in the design of various engineering systems, such as turbo-machinery, wind turbines, robotic manipulators and helicopter blades. The natural frequencies and mode shapes of such structures have been a topic of constant interest and hence received considerable attention. In helicopters, with the advancement in technology [1], the external hydraulic damper in the blade is replaced by incorporating a specialised elastomer with a high loss factor [2, 3]. The mechanical arrangement of the elastomeric damper leads to non-linear constraint during the deformation of the blade. Consequently, the dynamic analysis [4] becomes complicated due to the multiple load path and the highly non-linear characteristics of the elastomeric damper.

Beam theories for moderate deformation have been developed by several researchers [5–8]. These theories were validated by static tests performed using isotropic beams [9]. One of the earliest analytical models for bearingless rotors was

0022–460X/99/060001 + 25 $30.00/0

developed by Hodges [10, 11]; but the elastomeric damper was not included in the model. Chopra and his associates [12–14] reported several studies using finite element method to determine the periodic response and stability of a bearingless rotor in forward flight. Recently, Gandhi and Chopra [15] developed a non-linear damper model for the elastomeric bearing and examined its influence on the aeroelastic and aeromechanical stability of bearingless rotors.

Since the elastomeric damper has a strong influence on the structural dynamic characteristics of the bearingless rotor blades [1], development of an accurate model for the elastomer is essential. In 1970, the experiments conducted at Lord Corporation [3] first focussed on characterising the non-linear behaviour of the elastomers. Housmann [16] described the non-linear viscoelastic behaviour of an elastomer in terms of strain–amplitude dependent complex moduli. Felker *et al*. [17] carried out experiments to determine the properties of an elastomeric lag damper used in the Bell Model 412 helicopter. They also proposed a model in which both the stiffness and damping characteristics were expressed as a function of displacement. Smith *et al*. [18] developed a new damper model based on the method of Anelastic Displacement Fields (ADF), which generated viscoelastic finite elements in the time domain. Recently, a model comprising a series combination of a quartic spring and a linear Kelvin element has been proposed by Gandhi *et al*. [19]. In this model, the values of the parameters were determined by using the experimentally obtained values of complex moduli.

Independent of the above studies related to helicopter blades, several researchers have made significant contribution to the study of non-linear dynamics of beams using perturbation techniques. Anderson [20] formulated the non-linear equation of motion of a rotating bar and obtained the natural frequencies from the linearised equation. Using a harmonic balance technique, the non-linear structural dynamic analysis of blade model was performed by Minguet and Dugundji [21]. Nayfeh *et al*. [22] proposed a numerical–perturbation method for the determination of non-linear response of a continuous beam having complicated boundary conditions. The non-linear response of a simply supported beam with an attached spring–mass system was also investigated by Pakdemirli and Nayfeh [23]. Nayfeh and Nayfeh [24] obtained the non-linear modes and frequencies of a simply supported Euler–Bernoulli beam resting on an elastic foundation having quadratic and cubic non-linearities. Recently, non-linear normal mode shapes were determined for a cantilever beam by using the method of multiple time scale [25].

Most of the studies on helicopter blades have focussed primarily on the linearised dynamic analysis. Very little information is available on the influence of the elastomer on the structural dynamic characteristics of a rotor blade when the elastomer is included as a subsystem.

The major objectives of the present paper are to: (1) formulate a simple non-linear model to represent the characteristics of the elastomer which is amenable for subsequent integration into the non-linear analysis of rotor blade dynamics; (2) derive a closed form expression for the amplitude–frequency relationship of a rotating beam under transverse vibration with a non-linear

elastomeric constraint; (3) validate the results of the linear analysis using two different techniques.

2. ELASTOMERIC DAMPER MODEL

In contrast to the conventional hydraulic dampers, elastomeric dampers contribute both damping and stiffness to the rotor system. In fact, the contribution of the elastomer to the rotor stiffness is often a critical design issue. Due to the viscoelastic nature of the material, damping and stiffness are complex functions of the displacement amplitude, frequency and even temperature. Consequently, the development of a non-linear damper model that can be easily integrated with a structural dynamic analysis is essential.

It should be possible to represent a non-linear viscoelastic material by a combination of linear and non-linear restoring and dissipative elements. Since the static stress–strain curve of an elastomeric material is non-linear, it is logical to assume the restoring element to be non-linear. The experimental results of the single frequency bench test [17] of an elastomer lag damper show that both storage (G') and loss (G'') moduli decrease as the amplitude of motion increases, but neither of them display any significant dependence on frequency within the range of interest. Consequently, a Coulomb damper and a hysteretic damper are included in the model. Since the damping force is very high at low amplitude of motion, a Coulomb damper is chosen. If one replaces the hysteretic damper by a viscous damper, then the loss modulus would be frequency dependent which is not revealed by the experimental results. To keep the model simple, the spring and the damper are arranged in parallel. Figure 1 represents the viscoelastic solid model consisting of a non-linear spring, a Coulomb damper and a hysteretic damper.

The authors ultimate objective is to integrate the elastomer model with the dynamics of the rotating blade and study the combined system for the flap bending motion. Therefore, the following force–deformation relationship is proposed:

$$F_S = K_1 x - K_3 x^3 + K_5 x^5 - K_7 x^7, \tag{1}$$

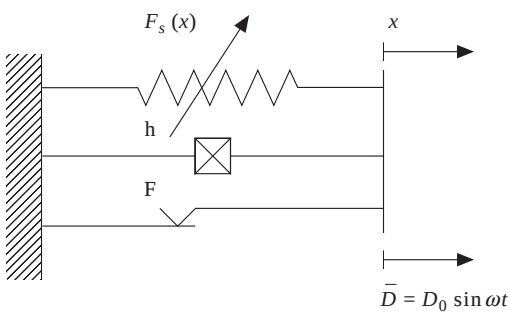

Figure 1. Elastomer model.

where F_S is the force exerted by the restoring element under a deformation x with K_1, K_3, K_5 and K_7 as constants. The constitutive differential equation with harmonic loading is now given by

$$K_1 x - K_3 x^3 + K_5 x^5 - K_7 x^7 + F \operatorname{sgn} |\dot{x}| + (h/\omega)\dot{x} = D_0 \sin \omega t, \tag{2}$$

where F and h are the Coulomb and hysteretic damping coefficients respectively. The following procedure is adopted to identify the system parameters, namely, K_1, K_3, K_5, K_7, F and h.

2.1. SYSTEM IDENTIFICATION

The steady state solution of equation (2) is assumed to be of the form

$$x = X \sin (\omega t - \phi). \tag{3}$$

Equation (3) is substituted into equation (2) and $D_0 \sin \omega t$ rewritten as $D_0[\sin (\omega t - \phi) \cos \phi + \cos (\omega t - \phi) \sin \phi]$. Thereafter, equating the coefficients of the first harmonic from both sides, one obtains

$$K_1 X - \tfrac{3}{4} K_3 X^3 + \tfrac{5}{8} K_5 X^5 - \tfrac{1}{2} K_7 X^7 = D_0 \cos \phi, \qquad 4F/\pi + hX = D_0 \sin \phi \tag{4, 5}$$

Equation (3) can be rewritten as

$$x = X_C \cos \omega t + X_S \sin \omega t, \tag{6}$$

where

$$X_C = -X \sin \phi, \qquad X_S = X \cos \phi. \tag{7}$$

Hence the real part G' and the imaginary part G'' of the complex moduli are given respectively, by

$$G' = D_0 |X_S| / (X_C^2 + X_S^2) = K_1 - \tfrac{3}{4} K_3 X^2 + \tfrac{5}{8} K_5 X^4 - \tfrac{1}{2} K_7 X^6, \tag{8}$$

$$G'' = D_0 |X_C| / (X_C^2 + X_S^2) = 4F/\pi X + h. \tag{9}$$

The values of G' and G'' for different amplitudes of motion can be obtained experimentally [17]. Let these be denoted by $G'(X)$ and $G''(X)$ respectively where X is the amplitude of motion. In order to determine the values of the stiffness parameters K_1, K_3, K_5 and K_7, one seeks to minimise the function

$$\Phi = \sum_{i=1}^{N} [F_i(X)]^2, \tag{10}$$

where

$$F_i(X) = K_1 - \tfrac{3}{4} K_3 X^2 + \tfrac{5}{8} K_5 X^4 - \tfrac{1}{2} K_7 X^6 - G'(X)$$

and N denotes the number of experimental data points used. Similarly, the values of the damping parameters F and h are obtained by minimising

$$\Psi = \sum_{j=1}^{N} [F_j(X)]^2 \tag{11}$$

TABLE 1

System parameters for the elastomeric damper model

System parameter	Fifth order approximation	Seventh order approximation
K_1 (N/m)	$2{\cdot}543437 \times 10^6$	$2{\cdot}673989 \times 10^6$
K_3 (N/m^3)	$8{\cdot}430654 \times 10^{11}$	$1{\cdot}315287 \times 10^{12}$
K_5 (N/m^5)	$1{\cdot}084698 \times 10^{17}$	$3{\cdot}519586 \times 10^{17}$
K_7 (N/m^7)	–	$3{\cdot}176266 \times 10^{22}$
F (N)	$4{\cdot}797347 \times 10^2$	$4{\cdot}797347 \times 10^2$
h (N/m)	$4{\cdot}569120 \times 10^5$	$4{\cdot}569120 \times 10^5$

with

$$F_j(X) = 4F/\pi X + h - G''(X)$$

The Nag Fortran Library routine based on a Gauss–Newton algorithm is used for the above minimisation problem. Proper scaling of data, specially the amplitude of excitation, has a significant influence on the performance of the optimization method. Number of data points N is taken to be 6. The system parameters so obtained are given in Table 1. The experimental data, given in FPS units in reference [17], have been converted to SI units. The comparison of the proposed model with the experimental data is shown in Figures 2 and 3. A fifth order approximation of the non-linear spring is also considered, and the corresponding stiffness curve is obtained following the same procedure. From Figure 2, it is observed that the seventh order approximation provides a better fit compared to the fifth order approximation.

3. BEARINGLESS ROTOR MODEL

A schematic diagram of the bearingless rotor is shown in Figure 4. The main rotor blade is attached to the hub through a flexbeam. Surrounding the flexbeam, there is a stiff torque tube which is attached to the main blade and the flexbeam

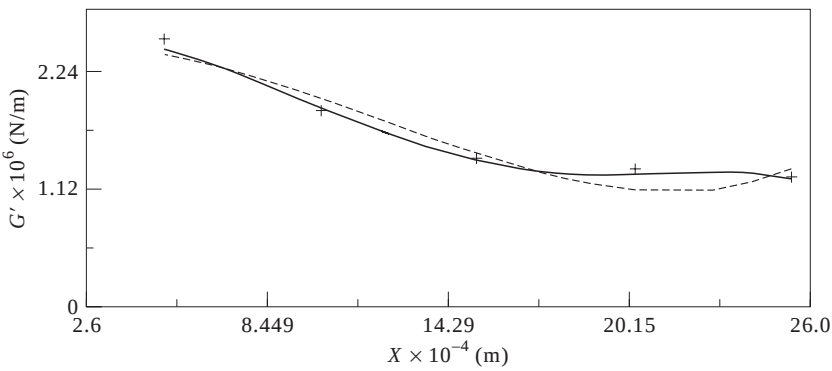

Figure 2. Variation of G' (storage modulus) with amplitude: +, experimental data; ——, seventh order spring model; – – –, fifth order spring model.

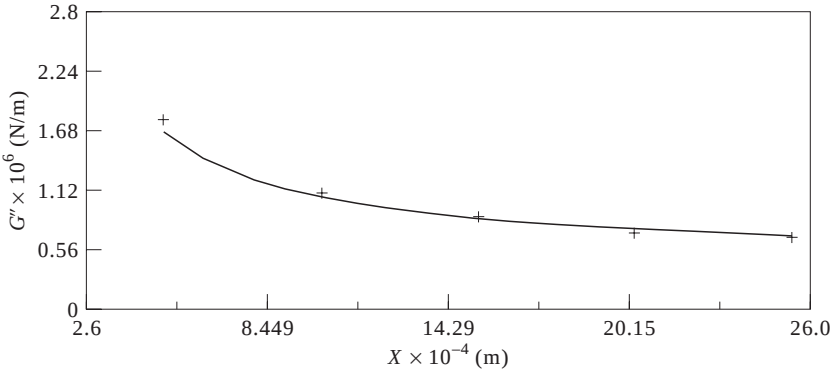

Figure 3. Variation of G'' (loss modulus) with amplitude: +, experimental data; ——, proposed model.

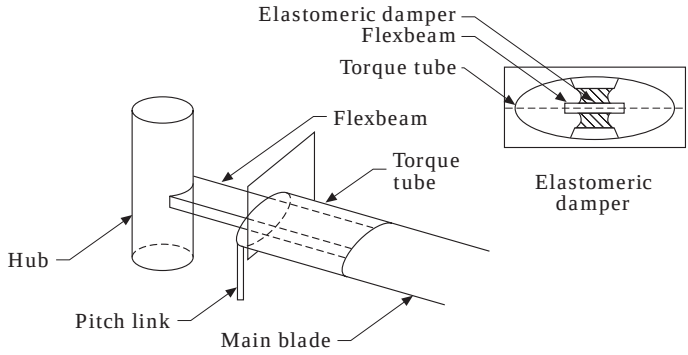

Figure 4. A schematic diagram of the bearingless rotor.

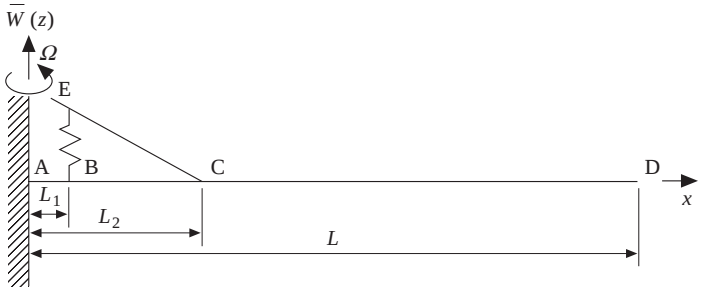

Figure 5. Idealised bearingless rotor.

at the outboard end and a pitch link at the inboard end. Pitch control is achieved by rotating the torque tube which in turn twists the flexbeam. An elastomeric damper is placed between the torque tube and the flexbeam to have adequate lag damping. It also serves the purpose of a spacer between the torque tube and the flexbeam. A simplified model of the bearingless rotor is shown in Figure 5 in which the torque tube is represented by a massless rigid link EC. The blade is assumed to be an Euler–Bernoulli beam with uniform cross-section and flexural rigidity. Since damping does not play any significant role as far as the natural frequencies

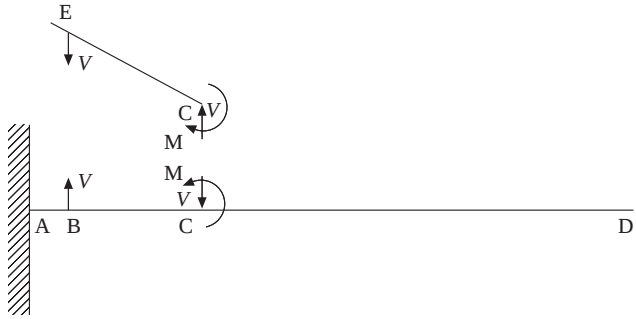

Figure 6. Free body diagrams of the bearingless rotor and the torque tube.

are concerned, elastomer connection is represented only by a spring element. The pitch link is also eliminated. Thus, the bearingless rotor can be idealised as a rotating beam having a non-linear spring connected between the points B and C on the beam through the torque tube. In what follows, the free vibration analysis of the rotor blade system is discussed by assuming the spring to be first linear and then non-linear.

4. LINEAR ANALYSIS

The dynamics of a rotating beam differs from that of a non-rotating one due to the addition of centrifugal stiffness. The differential equations of motion for a rotating beam have variable coefficients while those for a non-rotating beam have constant coefficients. Additionally, in the present problem, there is a transverse constraint at the point B (Figure 5) in the form of a linear spring whose deformation depends not only on the deflection at B, but also on the deflection and slope at the point C.

In this section, the equation of motion and the associated boundary conditions for the transverse vibration of the rotating beam shown in Figure 5 are first considered. Then two different solution techniques, one based on power series expansion and the other based on the Rayleigh–Ritz principle are used to determine the natural frequencies and the mode shapes. Numerical results obtained from these two methods are compared.

TABLE 2

Data for the beam used to obtain the numerical results

m (Kg/m)	L (m)	$EI/m\Omega^2L^4$	r (m)	Ω (rad/s)
9·7	6·6	0·0106	0·5	32·8

TABLE 3

Natural frequencies of the rotating beam without the elastomer

Mode	Power series	Rayleigh–Ritz	Ref. [28]	Ref. [29]
1	1·1245	1·1244	1·125	1·1247
2	3·4073	3·4073	–	3·4089
3	7·6218	7·6216	–	7·6376

4.1. POWER SERIES

By referring to Figure 5, the partial differential equations for small amplitude vibration of the rotating Euler–Bernoulli beam are

$$\left\{\begin{array}{lll} EI\dfrac{\partial^4 \bar{W}_1}{\partial x^4} - \tfrac{1}{2}m\Omega^2\dfrac{\partial}{\partial x}\left[(L^2-x^2)\dfrac{\partial \bar{W}_1}{\partial x}\right] + m\dfrac{\partial^2 \bar{W}_1}{\partial t^2} = 0 & \text{for} & 0 \leqslant x \leqslant L_1; \\ EI\dfrac{\partial^4 \bar{W}_2}{\partial x^4} - \tfrac{1}{2}m\Omega^2\dfrac{\partial}{\partial x}\left[(L^2-x^2)\dfrac{\partial \bar{W}_2}{\partial x}\right] + m\dfrac{\partial^2 \bar{W}_2}{\partial t^2} = 0 & \text{for} & L_1 \leqslant x \leqslant L_2; \\ EI\dfrac{\partial^4 \bar{W}_3}{\partial x^4} - \tfrac{1}{2}m\Omega^2\dfrac{\partial}{\partial x}\left[(L^2-x^2)\dfrac{\partial \bar{W}_3}{\partial x}\right] + m\dfrac{\partial^2 \bar{W}_3}{\partial t^2} = 0 & \text{for} & L_2 \leqslant x \leqslant L; \end{array}\right\} \tag{12}$$

where t denotes time, m denotes the mass per unit length, EI the flexural rigidity, Ω the angular velocity and $\bar{W}_i$ $(i = 1, 2, 3)$ the transverse deflection at different segments of the beam. By introducing the following dimensionless quantities

$$W_i = \bar{W}_i/L, \qquad \xi = x/L, \qquad \tau = \Omega t, \qquad \xi_i = L_i/L \tag{13}$$

and assuming a harmonic solution of the form

$$W_i(\xi, \tau) = W_i(\xi)\exp(i\omega\tau),$$

equations (12) reduce to

$$\left\{\begin{array}{lll} a\dfrac{\mathrm{d}^4 W_1}{\mathrm{d}\xi^4} - \dfrac{1}{2}\dfrac{\mathrm{d}}{\mathrm{d}\xi}\left[(1-\xi^2)\dfrac{\mathrm{d}W_1}{\mathrm{d}\xi}\right] - \omega^2 W_1 = 0 & \text{for} & 0 \leqslant \xi \leqslant \xi_1; \\ a\dfrac{\mathrm{d}^4 W_2}{\mathrm{d}\xi^4} - \dfrac{1}{2}\dfrac{\mathrm{d}}{\mathrm{d}\xi}\left[(1-\xi^2)\dfrac{\mathrm{d}W_2}{\mathrm{d}\xi}\right] - \omega^2 W_2 = 0 & \text{for} & \xi_1 \leqslant \xi \leqslant \xi_2; \\ a\dfrac{\mathrm{d}^4 W_3}{\mathrm{d}\xi^4} - \dfrac{1}{2}\dfrac{\mathrm{d}}{\mathrm{d}\xi}\left[(1-\xi^2)\dfrac{\mathrm{d}W_3}{\mathrm{d}\xi}\right] - \omega^2 W_3 = 0 & \text{for} & \xi_2 \leqslant \xi \leqslant 1; \end{array}\right\}, \tag{14}$$

where $a = EI/m\Omega^2 L^4$. In the present analysis, it is assumed that the beam is clamped at $\xi = 0$ and free at $\xi = 1$, so that the end boundary conditions are

$$W_1(0) = 0, \qquad \mathrm{d}W_1(0)/\mathrm{d}\xi = 0 \qquad \mathrm{d}^2 W_3(1)/\mathrm{d}\xi^2 = 0, \qquad \mathrm{d}^3 W_3(1)/\mathrm{d}\xi^3 = 0. \tag{15}$$

The free body diagrams of the beam AD and the link EC, shown in Figure 6 are considered where V and M are the force and the moment acting on EC and AD. Assuming the transverse deflection to be positive along Z direction, V and M are given by

$$V = K_1 \Delta \quad \text{and} \quad M = V(\xi_2 - \xi_1); \tag{16}$$

where $\Delta = [W_C - (\xi_2 - \xi_1)W'_C - W_B]$ is the extension of the spring, with W_C the deflection of the beam at C, W_B the deflection of the beam at B, W'_C the slope of the beam at C, and K_1 the linear stiffness of the spring.

In addition, one has to satisfy the conditions at the locations B and C, which after using equations (16) can be put in the following form:

$$W_1(\xi_1) = W_2(\xi_1), \qquad \mathrm{d}W_1(\xi_1)/\mathrm{d}\xi = \mathrm{d}W_2(\xi_1)/\mathrm{d}\xi,$$

$$\mathrm{d}^2W_1(\xi_1)/\mathrm{d}\xi^2 = \mathrm{d}^2W_2(\xi_1)/\mathrm{d}\xi^2;$$

$$\frac{\mathrm{d}^3W_1(\xi_1)}{\mathrm{d}\xi^3} + K^*\left[W_2(\xi_2) - (\xi_2 - \xi_1)\frac{\mathrm{d}W_2(\xi_2)}{\mathrm{d}\xi} - W_1(\xi_1) \right] = \frac{\mathrm{d}^3W_2(\xi_1)}{\mathrm{d}\xi^3}; \tag{17}$$

$$W_2(\xi_2) = W_3(\xi_2), \qquad \mathrm{d}W_2(\xi_2)/\mathrm{d}\xi = \mathrm{d}W_3(\xi_2)/\mathrm{d}\xi,$$

$$\frac{\mathrm{d}^2W_2(\xi_2)}{\mathrm{d}\xi^2} + K^*(\xi_2 - \xi_1)\left[W_2(\xi_2) - (\xi_2 - \xi_1)\frac{\mathrm{d}W_2(\xi_2)}{\mathrm{d}\xi} - W_1(\xi_1) \right] = \frac{\mathrm{d}^2W_3(\xi_2)}{\mathrm{d}\xi^2}$$

$$\frac{\mathrm{d}^3W_2(\xi_2)}{\mathrm{d}\xi^3} - K^*\left[W_2(\xi_2) - (\xi_2 - \xi_1)\frac{\mathrm{d}W_2(\xi_2)}{\mathrm{d}\xi} - W_1(\xi_1) \right] = \frac{\mathrm{d}^3W_3(\xi_2)}{\mathrm{d}\xi^3} \tag{18}$$

where $K^* = K_1L^3/EI$.

Equations (14) are linear ordinary differential equations with variable coefficients. Their solutions can be expressed as power series in the independent variable ξ as

$$W_1(\xi) = \sum_{k=1}^{\infty} C_k \xi^{k-1} \qquad \text{for} \qquad 0 \leqslant \xi \leqslant \xi_1;$$

$$W_2(\xi) = \sum_{k=1}^{\infty} D_k \xi^{k-1} \qquad \text{for} \qquad \xi_1 \leqslant \xi \leqslant \xi_2; \tag{19}$$

$$W_3(\xi) = \sum_{k=1}^{\infty} E_k \xi^{k-1} \qquad \text{for} \qquad \xi_2 \leqslant \xi \leqslant 1;$$

Inserting equations (19) into equations (14) and equating the coefficients of the like powers of ξ, the following recurrence relations are obtained after some algebraic manipulations:

$$2a(k+3)(k+2)(k+1)kC_{k+4} - (k+1)kC_k + [k(k-1) - 2\omega^2]C_k = 0,$$

$$2a(k+3)(k+2)(k+1)kD_{k+4} - (k+1)kD_k + [k(k-1) - 2\omega^2]D_k = 0,$$

$$2a(k+3)(k+2)(k+1)kE_{k+4} - (k+1)kE_k + [k(k-1) - 2\omega^2]E_k = 0,$$

$$\text{for } k = 1, 2, 3, \ldots, \tag{20}$$

Similarly, inserting the expressions (19) into the boundary conditions (15), (17) and (18), one obtains

$$C_1 = 0, \quad C_2 = 0, \quad \sum_{k=1}^{\infty} E_k(k-1)(k-2) = 0, \quad \sum_{k=1}^{\infty} E_k(k-1)(k-2)(k-3) = 0,$$

(21)

$$\sum_{k=1}^{\infty} C_k \xi_1^{k-1} - \sum_{k=1}^{\infty} D_k \xi_1^{k-1} = 0, \qquad \sum_{k=1}^{\infty} C_k(k-1)\xi_1^{k-2} - \sum_{k=1}^{\infty} D_k(k-1)\xi_1^{k-2} = 0,$$

$$\sum_{k=1}^{\infty} C_k(k-1)(k-2)\xi_1^{k-3} - \sum_{k=1}^{\infty} D_k(k-1)(k-2)\xi_1^{k-3} = 0,$$

$$\sum_{k=1}^{\infty} C_k(k-1)(k-2)(k-3)\xi_1^{k-4} + K^*$$

$$\left[\sum_{k=1}^{\infty} D_k \xi_2^{k-1} - (\xi_2 - \xi_1) \sum_{k=1}^{\infty} D_k(k-1)\xi_2^{k-2} - \sum_{k=1}^{\infty} C_k \xi_1^{k-1}\right]$$

$$- \sum_{k=1}^{\infty} D_k(k-1)(k-2)(k-3)\xi_1^{k-4} = 0; \tag{22}$$

and

$$\sum_{k=1}^{\infty} D_k \xi_2^{k-1} - \sum_{k=1}^{\infty} E_k \xi_2^{k-1} = 0, \qquad \sum_{k=1}^{\infty} D_k (k-1) \xi_2^{k-2} - \sum_{k=1}^{\infty} E_k (k-1) \xi_2^{k-2} = 0,$$

$$\sum_{k=1}^{\infty} D_k (k-1)(k-2) \xi_2^{k-3} + K^*(\xi_2 - \xi_1)$$

$$\times \left[\sum_{k=1}^{\infty} D_k \xi_2^{k-1} - (\xi_2 - \xi_1) \sum_{k=1}^{\infty} D_k (k-1) \xi_2^{k-2} - \sum_{k=1}^{\infty} C_k \xi_1^{k-1} \right]$$

$$- \sum_{k=1}^{\infty} E_k (k-1)(k-2) \xi_2^{k-3} = 0,$$

$$\sum_{k=1}^{\infty} D_k (k-1)(k-2)(k-3) \xi_2^{k-4} - K^*$$

$$\times \left[\sum_{k=1}^{\infty} D_k \xi_2^{k-1} - (\xi_2 - \xi_1) \sum_{k=1}^{\infty} D_k (k-1) \xi_2^{k-2} - \sum_{k=1}^{\infty} C_k \xi_1^{k-1} \right]$$

$$- \sum_{k=1}^{\infty} E_k (k-1)(k-2)(k-3) \xi_2^{k-4} = 0. \tag{23}$$

If the power series is truncated at the Pth term, then there are altogether $3P$ unknown coefficients. From the recurrence relations (20) and the boundary conditions (21)–(23) one obtains $3P$ simultaneous linear homogeneous equations. For a non-trivial solution, the determinant of the coefficient matrix must vanish. Thus, setting this determinant equal to zero one gets the frequency equation which is solved numerically for unknown ω. In order to obtain the mode shape, an additional normalising condition

$$W(1) = 1 \tag{24}$$

is imposed.

4.2. RAYLEIGH–RITZ METHOD

Since the blade is very stiff in the axial direction, the longitudinal elastic motion of the blade can be neglected. The axial force $P(x, t)$ at any point x is then only due to the centrifugal force. Therefore,

$$P(x, t) = \int_x^L m\Omega^2 s \, \mathrm{d}s = \tfrac{1}{2} m\Omega^2 L^2 \left(1 - \frac{x^2}{L^2} \right). \tag{25}$$

The kinetic energy of the entire beam is given by

$$T(t) = \tfrac{1}{2}\int_0^L m\left[\frac{\partial \bar{W}}{\partial t}\right]^2 \mathrm{d}x. \tag{26}$$

In the absence of any transverse load, the strain energy must include the effects of the bending moment, axial force and spring deformation. The expression for strain energy due to bending and the centrifugal force is

$$U_1 = \tfrac{1}{2}\int_0^L EI\left[\frac{\partial^2 \bar{W}(x,t)}{\partial x^2}\right]^2 \mathrm{d}x + \tfrac{1}{2}\int_0^L P(x,t)\left[\frac{\partial \bar{W}(x,t)}{\partial x}\right]^2 \mathrm{d}x. \tag{27}$$

Strain energy of the spring due to deformation Δ is

$$U_2 = \tfrac{1}{2}K_1\Delta^2, \tag{28}$$

where

$$\Delta = [\bar{W}(L_2,t) - (L_2 - L_1)\,\partial\bar{W}(L_2,t)/\partial x - \bar{W}(L_1,t)].$$

Hence the total strain energy of the system is

$$U = U_1 + U_2. \tag{29}$$

In order to derive the equation of motion, one introduces the dimensionless quantities defined by equations (13) and assumes a solution in the form

$$W(\xi,\tau) = \sum_{i=1}^{n} \phi_i(\xi) q_i(\tau), \tag{30}$$

where $q_i(\tau)$ are the generalised co-ordinates to be determined.

Substitution of equation (30) into equation (28) yields

$$U_2 = \tfrac{1}{2}K_1 L^2\left[\sum_{i=1}^{n} \psi_i q_i(\tau)\right]^2, \tag{31}$$

where

$$\psi_i = \phi_i(\xi_2) - (\xi_2 - \xi_1)\phi_i'(\xi_2) - \phi_i(\xi_1).$$

The quantity ψ_i can be interpreted as the deformation of the spring in the ith mode.

Introducing equations (26), (29), (30) and (13) into variational principle

$$\delta\int_{t_1}^{t_2} (T - U)\,\mathrm{d}t = 0 \tag{32}$$

and collecting appropriate terms, one obtains

$$\sum_{i=1}^{n}\left[\int_0^1 \phi_i\phi_r \,\mathrm{d}\xi\right]\ddot{q}_i(\tau) + \sum_{i=1}^{n}\left[\int_0^1 \frac{EI}{m\Omega^2L^4}\,\phi_i''\phi_r'' \,\mathrm{d}\xi\right.$$

$$\left. + \int_0^1 \tfrac{1}{2}(1-\xi^2)\phi_i'\phi_r' \,\mathrm{d}\xi + \frac{K_1}{m\Omega^2L}\,\psi_i\psi_r\right]q_i(\tau) = 0, \qquad r = 1, 2, 3, \ldots.$$

Therefore, the eigenvalue problem can be formed as

$$[\mathbf{M}]\{\ddot{q}\} + [\mathbf{K}]\{q\} = 0, \tag{33}$$

where

$$[\mathbf{K}] = \int_0^1 a\phi_i''\phi_r'' \,\mathrm{d}\xi + \int_0^1 \tfrac{1}{2}(1-\xi^2)\phi_i'\,\phi_r' \,\mathrm{d}\xi + \alpha_1\psi_i\psi_r,$$

$$[\mathbf{M}] = \int_0^1 \phi_i\phi_r \,\mathrm{d}\xi, \qquad a = EI/m\Omega^2L^4, \qquad \alpha_1 = K_1/m\Omega^2L.$$

Since the assumed modes are not orthogonal to one another, the mass and stiffness matrices corresponding to equation (33) are fully populated resulting in coupled equations of motion. The above eigenvalue problem is solved numerically to determine the natural frequencies.

5. NON-LINEAR ANALYSIS

By considering a non-linear spring to represent the elastomer and following Nayfeh [23], a numerical–perturbation technique can be adopted for the non-linear analysis of the rotor blade. Accordingly, the continuous system has to be first discretized by any method of weighted residuals [26] (such as collocation, Galerkin, Rayleigh–Ritz etc.); to obtain a system of coupled non-linear ordinary differential equations. Then, one can apply any of the perturbation techniques. Although the Galerkin discretisation procedure is most common, the authors have followed the Rayleigh–Ritz technique since it gives a symmetric stiffness matrix for this problem whereas the Galerkin procedure leads to a non-symmetric matrix.

5.1. NON-LINEAR EQUATION OF MOTION

When the elastomer is represented by the non-linear spring, the expression for strain energy of the spring is modified as

$$U_2 = \tfrac{1}{2}K_1\Delta^2 - \tfrac{1}{4}K_3\Delta^4 + \tfrac{1}{6}K_5\Delta^6 - \tfrac{1}{8}K_7\Delta^8. \tag{34}$$

By introducing the following dimensionless terms

$$W = \bar{W}/\gamma^4L, \qquad \xi = x/L, \qquad \tau = \Omega t, \tag{35}$$

with $\gamma = r/L(\ll 1)$, where r is the radius of gyration of the beam cross-section about the neutral axis, one can rewrite equation (34) as

$$U_2 = \tfrac{1}{2}K_1L^2\epsilon\left[\sum_{i=1}^{n}\psi_i q_i(\tau)\right]^2 - \tfrac{1}{4}K_3L^4\epsilon^2\left[\sum_{i=1}^{n}\psi_i q_i(\tau)\right]^4$$

$$+\tfrac{1}{6}K_5L^6\epsilon^3\left[\sum_{i=1}^{n}\psi_i q_i(\tau)\right]^6 - \tfrac{1}{8}K_7L^8\epsilon^4\left[\sum_{i=1}^{n}\psi_i q_i(\tau)\right]^8, \tag{36}$$

where $\epsilon = \gamma^8$ is a small parameter. Using equation (36), instead of equation (31) and following the procedure outlined in section 4.2, one obtains the temporal equation of motion as

$$[\mathbf{M}]\{\ddot{\mathbf{q}}\} + [\mathbf{K}]\{\mathbf{q}\} + \mathbf{F}_{NL}\{\mathbf{q}\} = 0, \tag{37}$$

where $\mathbf{F}_{NL}\{\mathbf{q}\}$ contains the contribution of the non-linear terms in the spring force. In order to decouple the linear part of the above equation, the following linear transformation is introduced

$$q_i(\tau) = [\mathbf{P}]z_i(\tau), \tag{38}$$

where $[\mathbf{P}]$ is formed by the eigenvector of the linear eigenvalue problem obtained after neglecting the non-linear terms in equation (37).

Therefore, the assumed mode solution given in equation (30) is modified as

$$W(\xi, \tau) = \sum_{i=1}^{n}\overline{\phi}_i(\xi)z_i(\tau), \tag{39}$$

where

$$\overline{\phi}_i = \phi_1 p_{1i} + \phi_2 p_{2i} + \cdots + \phi_n p_{ni}, \tag{40}$$

with p_{ij} as the elements of the matrix $[\mathbf{P}]$. In equation (36), $\psi_i q_i(\tau)$ will be replaced by $\overline{\psi}_i z_i(\tau)$, where

$$\overline{\psi}_i = \psi_1 p_{1i} + \psi_2 p_{2i} + \cdots + \psi_n p_{ni}. \tag{41}$$

Using equation (35) and applying the variational principle, one obtains the temporal equation in the form

$$\ddot{z}_i(\tau) + \omega_i^2 z_i(\tau) - \epsilon\alpha_3\sum_{m=1}^{n}\sum_{s=1}^{n}\sum_{r=1}^{n}\Gamma_{imsr}z_m z_s z_r$$

$$+\epsilon^2\alpha_5\sum_{m=1}^{n}\sum_{s=1}^{n}\sum_{r=1}^{n}\sum_{t=1}^{n}\sum_{u=1}^{n}\Gamma_{imsrtu}z_m z_s z_r z_t z_u$$

$$-\epsilon^3\alpha_7\sum_{m=1}^{n}\sum_{s=1}^{n}\sum_{r=1}^{n}\sum_{t=1}^{n}\sum_{u=1}^{n}\sum_{v=1}^{n}\sum_{w=1}^{n}\Gamma_{imsrtuvw}z_m z_s z_r z_t z_u z_v z_w = 0,$$

$$i = 1, 2, 3, \ldots, n \tag{42}$$

where ω_i is ith linear natural frequency and

$$\Gamma_{imsr} = \overline{\psi}_i\overline{\psi}_m\overline{\psi}_s\overline{\psi}_r, \qquad \Gamma_{imsrtu} = \overline{\psi}_i\overline{\psi}_m\overline{\psi}_s\overline{\psi}_r\overline{\psi}_t\overline{\psi}_u,$$

$$\Gamma_{imsrtuvw} = \overline{\psi}_i\overline{\psi}_m\overline{\psi}_s\overline{\psi}_r\overline{\psi}_t\overline{\psi}_u\overline{\psi}_v\overline{\psi}_w,$$

$$\alpha_3 = K_3L/m\Omega^2, \qquad \alpha_5 = K_5L^3/m\Omega^2, \qquad \alpha_7 = K_7L^5/m\Omega^2, \tag{43}$$

The linear part of equation (42) is no longer coupled. Now, one uses the method of multiple scales and seeks an expansion of the solution of equation (42) for small but finite amplitude in the form

$$z_i(\tau;\epsilon) = z_{i0}(T_0, T_1, T_2, T_3) + \epsilon z_{i1}(T_0, T_1, T_2, T_3) + \epsilon^2 z_{i2}(T_0, T_1, T_2, T_3) + \cdots; \tag{44}$$

where ϵ is a small non-dimensional parameter.

Different time scales are introduced as

$$T_n = \epsilon_n\tau, \qquad n = 0, 1, 2, \ldots. \tag{45}$$

Here T_0 is a fast scale associated with the changes occurring with frequencies near ω_i, while T_n for $n \geqslant 1$ are slow scales associated with changes that can only be noticed after several cycles. In terms of usual operator notations, one can write

$$\mathrm{d}/\mathrm{d}\tau = D_0 + \epsilon D_1 + \epsilon^2 D_2 + \epsilon^3 D_3 + \cdots, \tag{46}$$

$$\mathrm{d}^2/\mathrm{d}\tau^2 = D_0^2 + 2\epsilon D_0D_1 + \epsilon^2(2D_0D_1 + D_1^2) + \epsilon^3(2D_0D_3 + 2D_1D_2) + \cdots, \tag{47}$$

where $D_i = \mathrm{d}/\mathrm{d}T_i$, $i = 0, 1, 2, \ldots$. Substituting equations (44) and (47) into equation (42) and equating the coefficients of like powers of ϵ, one has

$$\epsilon^0: D_0^2z_{i0} + \omega_i^2z_{i0} = 0, \qquad \epsilon^1: D_0^2z_{i1} + \omega_i^2z_{i1} = -2D_0D_1z_{i0} + \alpha_3\Gamma_{4i}z_{i0}^3, \tag{48, 49}$$

$$\epsilon^2: D_0^2z_{i2} + \omega_i^2z_{i2} = -2D_0D_1z_{i1} - D_1^2z_{i0} - 2D_0D_2z_{i0} + 3\alpha_3\Gamma_{4i}z_{i0}^2z_{i1} - \alpha_5\Gamma_{6i}z_{i0}^5, \tag{50}$$

$$\epsilon^3: D_0^2z_{i3} + \omega_i^2z_{i3} = -2D_0D_1z_{i2} - D_1^2z_{i1} - 2D_0D_2z_{i1} - 2D_0D_3z_{i0} - 2D_1D_2z_{i0} + 3\alpha_3\Gamma_{4i}z_{i0}^2z_{i2} + 3\alpha_3\Gamma_{4i}z_{i0}z_{i1}^2 - 5\alpha_5\Gamma_{6i}z_{i0}^4z_{i1} + \alpha_7\Gamma_{8i}z_{i0}^7, \tag{51}$$

where

$$\Gamma_{4i} = (\overline{\psi}_i)^4, \qquad \Gamma_{6i} = (\overline{\psi}_i)^6, \qquad \Gamma_{8i} = (\overline{\psi}_i)^8. \tag{52}$$

One assumes the solution of equation (48) as

$$z_{i0} = A_i(T_1, T_2, T_3)\,\mathrm{e}^{\mathrm{i}\omega_iT_0} + \overline{A}_i(T_1, T_2, T_3)\,\mathrm{e}^{-\mathrm{i}\omega_iT_0} \tag{53}$$

By substituting the first order solution given by equation (53) into equation (49), one obtains

$$D_0^2z_{i1} + \omega_i^2z_{i1} = -2\mathrm{i}\omega_iD_1(A_i)\,\mathrm{e}^{\mathrm{i}\omega_iT_0} + \alpha_3\Gamma_{4i}[A_i^3\,\mathrm{e}^{\mathrm{i}3\omega_iT_0} + 3A_i^2\overline{A}_i\,\mathrm{e}^{\mathrm{i}\omega_iT_0}] + \text{c.c.}, \tag{54}$$

where c.c. indicates the complex conjugate.

In order that z_{i1}/z_{i0} be bounded for all T_0, the secular terms must vanish. Hence

$$-2\mathrm{i}\omega_iD_1(A_i) + 3\alpha_3\Gamma_{4i}A_i^2\overline{A}_i = 0 \tag{55}$$

and the solution for z_{i1} becomes

$$z_{i1} = -(1/8\omega_i^2)\alpha_3\Gamma_{4i}A_i^3\,\mathrm{e}^{\mathrm{i}3\omega_i T_0} + \text{c.c.}. \tag{56}$$

In order to uniquely define the amplitude A_i of the fundamental frequency of oscillation, the homogeneous solution of equation (54) has not been included.

To solve equation (55), one assumes

$$A_i = \tfrac{1}{2}a_i\,\mathrm{e}^{\mathrm{i}\beta_i}, \tag{57}$$

where a_i and β_i are real functions of T_1, T_2, T_3. Substituting equation (57) into equation (55) and separating the real and imaginary parts, one obtains

$$\partial a_i/\partial T_1 = 0, \qquad \omega_i\,\partial\beta_i/\partial T_1 + \tfrac{3}{8}\alpha_3\Gamma_{4i}a_i^2 = 0.$$

Hence

$$a_i = a_i(T_2, T_3), \qquad \beta_i = -(3/8\omega_i)\alpha_3\Gamma_{4i}a_i^2 T_1 + \beta_i'(T_2, T_3). \tag{58}$$

Substitution of equations (53) and (56) into equation (50) yields

$$\begin{aligned} D_0^2 z_{i2} + \omega_i^2 z_{i2} &= (27/32\omega_i^2)\alpha_3^2\Gamma_{4i}^2 a_i^2 A_i^3\,\mathrm{e}^{\mathrm{i}3\omega_i T_0} + (9/64\omega_i^2)\alpha_3^2\Gamma_{4i}^2 a_i^4 A_i\,\mathrm{e}^{\mathrm{i}\omega_i T_0} \\ &\quad - 2\mathrm{i}\omega_i D_2(A_i)\,\mathrm{e}^{\mathrm{i}\omega_i T_0} - (3/8\omega_i^2)\alpha_3^2\Gamma_{4i}^2 A_i^5\,\mathrm{e}^{\mathrm{i}5\omega_i T_0} - (3/8\omega_i^2)\alpha_3^2\Gamma_{4i}^2 A_i^3\overline{A}_i^2\,\mathrm{e}^{\mathrm{i}\omega_i T_0} \\ &\quad - (3/4\omega_i^2)\alpha_3^2\Gamma_{4i}^2 A_i^4\overline{A}_i\,\mathrm{e}^{\mathrm{i}3\omega_i T_0} \\ &\quad - \alpha_5\Gamma_{6i}(A_i^5\,\mathrm{e}^{\mathrm{i}5\omega_i T_0} + 5A_i^4\overline{A}_i\,\mathrm{e}^{\mathrm{i}3\omega_i T_0} + 10A_i^3\overline{A}_i^2\,\mathrm{e}^{\mathrm{i}\omega_i T_0}) + \text{c.c.}. \end{aligned} \tag{59}$$

Again the absence of any secular term in the solution of equation (59) requires

$$(9/128\omega_i^2)\alpha_3^2\Gamma_{4i}^2 a_i^5 - 2\mathrm{i}\omega_i D_2(A_i) - (3/8\omega_i^2)\alpha_3^2\Gamma_{4i}^2 A_i^3\overline{A}_i^2 - 10\alpha_5\Gamma_{6i}A_i^3\overline{A}_i^2 = 0 \tag{60}$$

Separating the real and imaginary parts, one has, after some algebraic manipulations,

$$\frac{\partial a_i}{\partial T_2} = 0, \qquad \frac{9}{128\omega_i^2}\,\alpha_3^2\Gamma_{4i}^2 a_i^5 + \omega_i a_i\,\frac{\partial\beta_i'}{\partial T_2} - \frac{3}{256\omega_i^2}\,\alpha_3^2\Gamma_{4i}^2 a_i^5 - \tfrac{5}{16}\alpha_5\Gamma_{6i}a_i^5 = 0.$$

Hence

$$a_i = a_i(T_3), \qquad \beta_i' = -(15/256\omega_i^3)\alpha_3^2\Gamma_{4i}^2 a_i^4 T_2 + (5/16\omega_i)\alpha_5\Gamma_{6i}a_i^4 T_2 + \beta_i''(T_3). \tag{61}$$

The solution of equation (59) is given by

$$\begin{aligned} z_{i2} &= -(27/256\omega_i^4)\alpha_3^2\Gamma_{4i}^2 a_i^2 A_i^3\,\mathrm{e}^{\mathrm{i}3\omega_i T_0} + (3/32\omega_i^4)\alpha_3^2\Gamma_{4i}^2 A_i^4\overline{A}_i\,\mathrm{e}^{\mathrm{i}3\omega_i T_0} \\ &\quad + (3/192\omega_i^4)\alpha_3^2\Gamma_{4i}^2 A_i^5\,\mathrm{e}^{\mathrm{i}5\omega_i T_0} + (1/24\omega_i^2)\alpha_5\Gamma_{6i}A_i^5\,\mathrm{e}^{\mathrm{i}5\omega_i T_0} \\ &\quad + (5/8\omega_i^2)\alpha_5\Gamma_{6i}A_i^4\overline{A}_i\,\mathrm{e}^{\mathrm{i}3\omega_i T_0} + \text{c.c.}. \end{aligned} \tag{62}$$

By substituting equations (53), (56) and (62) into equation (51), one has

$$D_0^2 z_{i3} + \omega_i^2 z_{i3} = -2D_0 D_1 \Bigg[-\frac{27}{256\omega_i^4}\alpha_3^2 \Gamma_{4i}^2 a_i^2 A_i^3 \, e^{i3\omega_i T_0} + \frac{3}{32\omega_i^4}\alpha_3^2 \Gamma_{4i}^2 A_i^4 \overline{A}_i \, e^{i3\omega_i T_0}$$

$$+ \frac{3}{192\omega_i^4}\alpha_3^2 \Gamma_{4i}^2 A_i^5 \, e^{i5\omega_i T_0} + \frac{1}{24\omega_i^2}\alpha_5 \Gamma_{6i} A_i^5 \, e^{i5\omega_i T_0}$$

$$+ \frac{5}{8\omega_i^2}\alpha_5 \Gamma_{6i} A_i^4 \overline{A}_i \, e^{i3\omega_i T_0} + \text{c.c.} \Bigg]$$

$$- 2D_0 D_2 \left(-\frac{1}{8\omega_i^2}\alpha_3 \Gamma_{4i} A_i^3 \, e^{i3\omega_i T_0} + \text{c.c.} \right)$$

$$- D_1^2 \left(-\frac{1}{8\omega_i^2}\alpha_3 \Gamma_{4i} A_i^3 \, e^{i3\omega_i T_0} + \text{c.c.} \right)$$

$$- 2D_0 D_3 (A_i \, e^{i\omega_i T_0} + \text{c.c.}) - 2D_1 D_2 (A_i \, e^{i\omega_i T_0} + \text{c.c.})$$

$$+ 3\alpha_3 \Gamma_{4i} (A_i \, e^{i\omega_i T_0} + \text{c.c.}) \left(-\frac{1}{8\omega_i^2}\alpha_3 \Gamma_{4i} A_i^3 \, e^{i3\omega_i T_0} + \text{c.c.} \right)^2$$

$$- 5\alpha_5 T_{6i} (A_i^4 \, e^{i4\omega_i T_0} + 4A_i^3 \overline{A}_i \, e^{i2\omega_i T_0} + 6A_i^2 \overline{A}_i^2 + \text{c.c.})$$

$$\times \left(-\frac{1}{8\omega_i^2}\alpha_3 \Gamma_{4i} A_i^3 \, e^{i3\omega_i T_0} + \text{c.c.} \right)$$

$$+ 3\alpha_3 \Gamma_{4i} (A_i^2 \, e^{i2\omega_i T_0} + 2A_i \overline{A}_i + \text{c.c.}) z_{i2} + \alpha_7 \Gamma_{8i} (A_i \, e^{i\omega_i T_0} + \text{c.c.})^7. \quad (63)$$

One does not seek the solution of equation (63). The condition for eliminating the secular term can be given, after some algebraic manipulations, as

$$-i\omega_i \frac{\partial a_i}{\partial T_3} + \omega_i a_i \frac{\partial \beta_i''}{\partial T_3} - \frac{5}{64\omega_i^2}\alpha_3 \Gamma_{4i} \alpha_5 \Gamma_{6i} a_i^7 + \frac{111}{64 \times 128\omega_i^4}\alpha_3^3 \Gamma_{4i}^3 a_i^7$$

$$+ \frac{35}{128\omega_i}\alpha_7 \Gamma_{8i} a_i^7 = 0. \quad (64)$$

Again, separating the real and imaginary parts of equation (64), one gets

$$\partial a_i / \partial T_3 = 0 \quad \text{or} \quad a_i = \text{constant};$$

$$\frac{\partial \beta_i''}{\partial T_3} = \frac{5}{64\omega_i^3}\alpha_3 \Gamma_{4i} \alpha_5 \Gamma_{6i} a_i^6 - \frac{111}{64 \times 128\omega_i^5}\alpha_3^3 \Gamma_{4i}^3 a_i^6 - \frac{35}{128\omega_i}\alpha_7 \Gamma_{8i} a_i^6$$

or

$$\beta_i'' = \frac{5}{64\omega_i^3}\alpha_3 \Gamma_{4i} \alpha_5 \Gamma_{6i} a_i^6 T_3 - \frac{111}{64 \times 128\omega_i^5}\alpha_3^3 \Gamma_{4i}^3 a_i^6 T_3 - \frac{35}{128\omega_i}\alpha_7 \Gamma_{8i} a_i^6 T_3 + \beta_0 = 0. \quad (65)$$

From equations (45), (58), (61) and (65) one can write the frequency–amplitude relationship as

$$\omega_{N_i} = \omega_i - \epsilon \frac{3}{8\omega_i} \alpha_3 \Gamma_{4i} a_i^2 - \epsilon^2 \frac{15}{256\omega_i^3} \alpha_3^2 \Gamma_{4i}^2 a_i^4 + \epsilon^2 \frac{5}{16\omega_i} \alpha_5 \Gamma_{6i} a_i^4$$

$$+ \epsilon^3 \frac{5}{64\omega_i^3} \alpha_3 \Gamma_{4i} \alpha_5 \Gamma_{6i} a_i^6 - \epsilon^3 \frac{111}{64 \times 128\omega_i^5} \alpha_3^3 \Gamma_{4i}^3 a_i^6 - \epsilon^3 \frac{35}{128\omega_i} \alpha_7 \Gamma_{8i} a_i^6; \tag{66}$$

where ω_{N_i} is the ith non-linear natural frequency. Redefining the amplitude as

$$\hat{A}_i = a_i / \sqrt{\epsilon} \tag{67}$$

One obtains the final frequency–amplitude relationship as

$$\omega_{N_i} = \omega_i - \frac{3}{8\omega_i} \alpha_3 \Gamma_{4i} \hat{A}_i^2 - \frac{15}{256\omega_i^3} \alpha_3^2 \Gamma_{4i}^2 \hat{A}_i^4 + \frac{5}{16\omega_i} \alpha_5 \Gamma_{6i} \hat{A}_i^4$$

$$+ \frac{5}{64\omega_i^3} \alpha_3 \Gamma_{4i} \alpha_5 \Gamma_{6i} \hat{A}_i^6 - \frac{111}{64 \times 128\omega_i^5} \alpha_3^3 \Gamma_{4i}^3 \hat{A}_i^6 - \frac{35}{128\omega_i} \alpha_7 \Gamma_{8i} \hat{A}_i^6. \tag{68}$$

6. RESULTS AND DISCUSSION

The numerical results obtained by using the methods outlined in sections 4 and 5 are presented below in three parts. The data used are given in Table 2.

6.1. ROTATING BEAM WITHOUT ELASTOMER

The natural frequencies and mode shapes of a rotating beam are obtained by using both the power series and the Rayleigh–Ritz method. The first three natural frequencies in the flap mode are calculated. The roots of the frequency equation obtained by the power series method are computed by an iterative search procedure. For Rayleigh–Ritz analysis, the following comparison functions [27] satisfying all the boundary conditions are used:

$$\phi_i(\xi) = \xi^i[\{(i+2)(i+3)/6\}\xi - \{i(i+3)/3\}\xi^2 + \{i(i+1)/6\}\xi^3], \tag{69}$$

where i refers to the mode number.

The results so obtained are given in Table 3. It is observed that the results obtained by both the methods are in excellent agreement with those presented in references [28,29].

6.2. ROTATING BEAM WITH LINEAR ELASTOMER

The elastomer is idealised as a linear spring. The dynamic characteristics of a rotating beam are analysed for different values of $\xi_1 (= L_1/L)$ and $\xi_2 (= L_2/L)$ (see Figure 5). Calculations are also performed for four values of the dimensionless spring constant $K^* = 1000$, 2000, 3000 and 4000. To validate the results, the frequencies are evaluated by using both the power series method and the Rayleigh–Ritz technique. The power series converges for $P = 50$, where P represents the number of terms in each series. Since the rotating beam is divided into three parts and each part is represented by a 50 term power series, there are

TABLE 4

Natural frequencies of the rotating beam with a linear elastomer

		$\xi_1 = 0{\cdot}10,\ \xi_2 = 0{\cdot}15$		$\xi_1 = 0{\cdot}10,\ \xi_2 = 0{\cdot}20$		$\xi_1 = 0{\cdot}10,\ \xi_2 = 0{\cdot}25$		$\xi_1 = 0{\cdot}10,\ \xi_2 = 0{\cdot}30$	
Mode	K^*	Power series	Rayleigh–Ritz	Power series	Rayleigh–Ritz	Power series	Rayleigh–Ritz	Power series	Rayleigh–Ritz
1	1000	1·125	1·125	1·127	1·127	1·130	1·131	1·133	1·134
2		3·407	3·407	3·409	3·409	3·407	3·407	3·413	3·416
3		7·617	7·622	7·628	7·635	7·716	7·763	7·960	8·152
1	2000	1·125	1·125	1·128	1·129	1·132	1·134	1·134	1·137
2		3·408	3·408	3·409	3·409	3·407	3·407	3·414	3·420
3		7·617	7·635	7·634	7·645	7·754	7·847	8·039	8·349
1	3000	1·125	1·125	1·130	1·131	1·133	1·136	1·135	1·138
2		3·409	3·408	3·410	3·411	3·407	3·407	3·415	3·422
3		7·618	7·622	7·639	7·656	7·774	7·903	8·075	8·449
1	4000	1·125	1·125	1·130	1·133	1·134	1·138	1·136	1·139
2		3·409	3·408	3·410	3·412	3·407	3·408	3·415	3·424
3		7·618	7·622	7·642	7·664	7·786	7·937	8·095	8·509

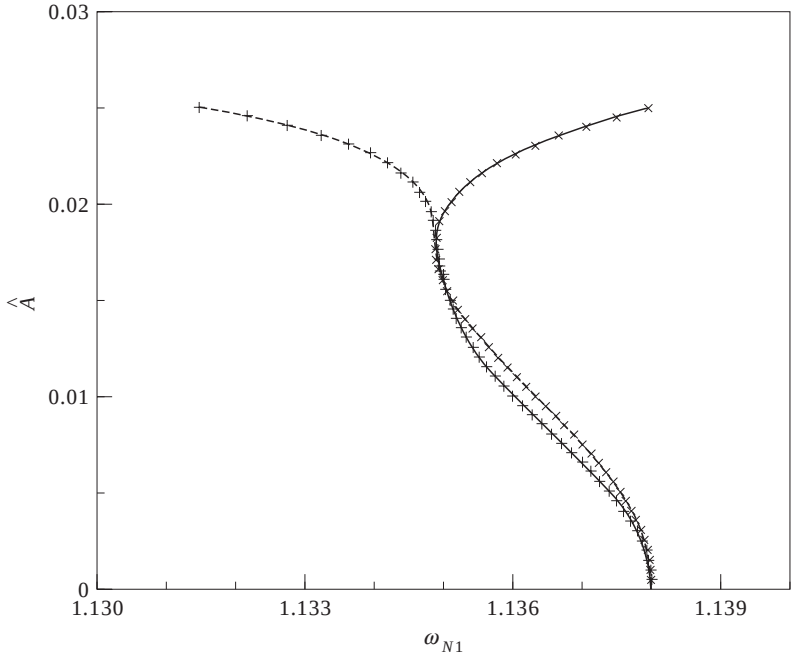

Figure 7. Variation of the first non-linear frequency with amplitude of oscillation: --×--, fifth order approximation; —+—, seventh order approximation.

in total 150 unknown coefficients. While using the Rayleigh–Ritz technique, the natural frequencies converged when sixteen comparison functions ($i = 1$–16 in equation (69)) were used. Table 4 presents the first three natural frequencies of the rotating beam, evaluated by both techniques, for different values of the parameters (K^*, ξ_2). In most of the cases, the natural frequencies obtained by both methods are in excellent agreement with each other. However, there is a difference of about 3–6% in the third natural frequency for $\xi_2 = 0{\cdot}3$. For a given configuration, say $\xi_1 = 0{\cdot}1$ and $\xi_2 = 0{\cdot}25$, when the stiffness (K^*) is varied from 1000–4000, the percentage variation in natural frequency in the first mode is 0·6%; in the second mode the variation is 0·02% and in the third mode the variation is 2·17%. Similar behaviour is also observed for other values of ξ_2.

6.3. NON-LINEAR ANALYSIS

The force–deformation characteristics of the non-linear spring are represented by two models: one with a fifth order approximation and the other with a seventh order approximation as detailed in section 2. For the fifth and seventh order approximations, one writes $F_S = K_1 x - K_3 x^3 + K_5 x^5$ and $F_S = K_1 x - K_3 x^3 + K_5 x^5 - K_7 x^7$ respectively.

For the fifth order approximation, corresponding to the value of K_1 given in Table 1, $K^* = 3480{\cdot}4$. Similarly for the seventh order approximation, $K^* = 3658{\cdot}8$. It should be noted that both these values are close to 4000 for which the numerical results with the linear analysis have already been presented. The non-linear dynamic analysis was carried out for a specific rotor blade

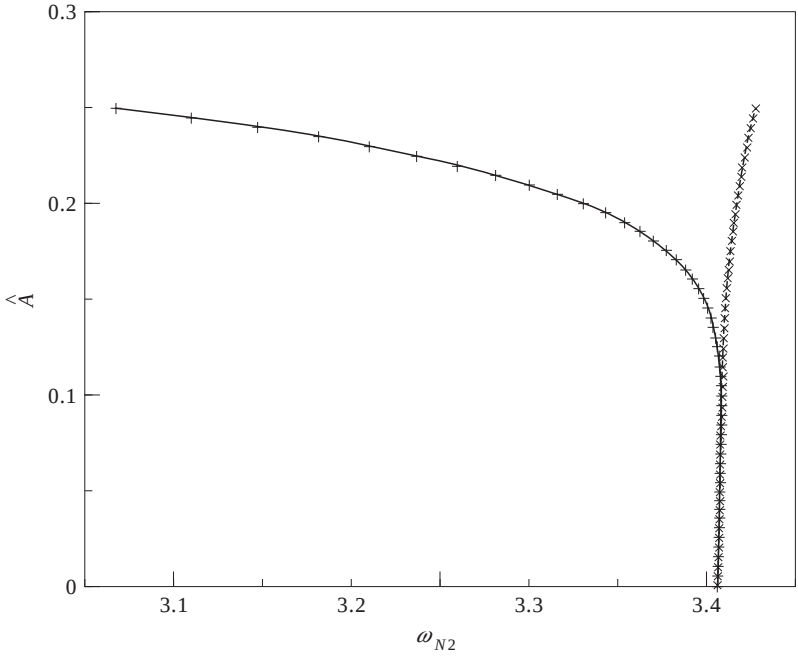

Figure 8. Variation of the second non-linear frequency with amplitude of oscillation: --×--, fifth order approximation; —+—, seventh order approximation.

configuration having $\xi_1 = 0{\cdot}1$ and $\xi_2 = 0{\cdot}25$. These are representative values corresponding to a realistic bearingless rotor.

The procedure of evaluating the frequency–amplitude (see equation (68)) relationship is as follows. Using the linear stiffness term from the non-linear

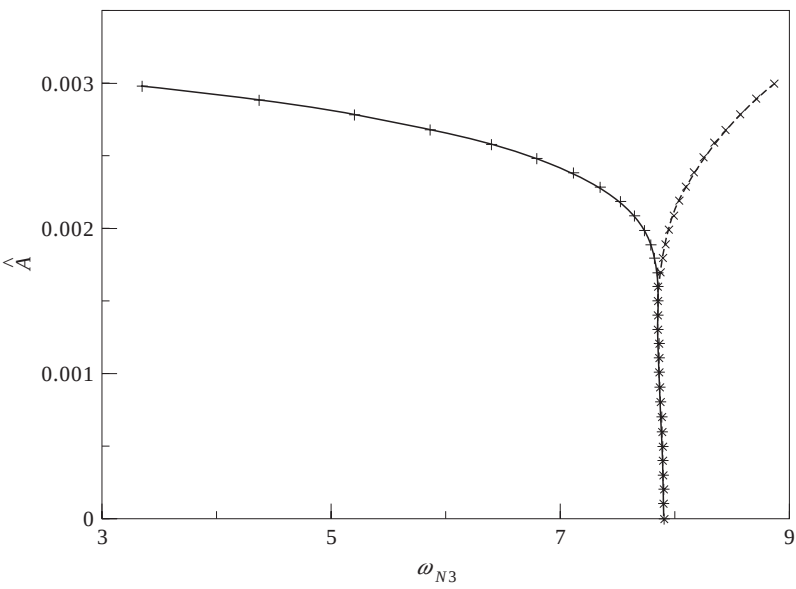

Figure 9. Variation of the third non-linear frequency with amplitude of oscillation: --×--, fifth order approximation; —+—, seventh order approximation.

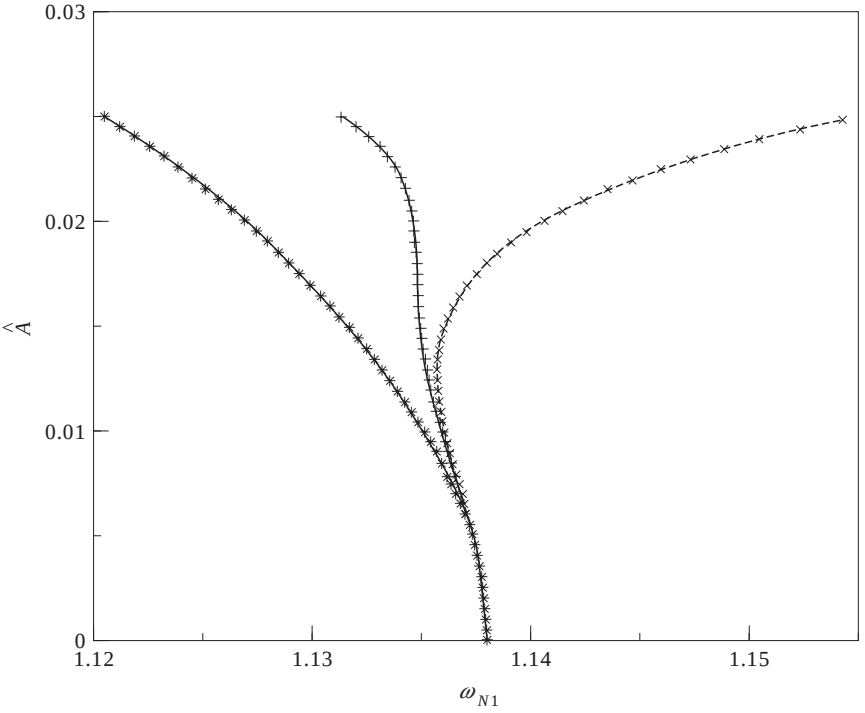

Figure 10. Influence of different orders of approximation on the first non-linear natural frequency: --∗--, third order approximation; --×--, fifth order approximation; —+—, seventh order approximation.

force–deformation relationship of the spring, a linear eigenvalue problem is solved for the natural frequencies, the transformation matrix [**P**] (equation (38)) and the linear mode shapes $\overline{\phi}_i$ (equation (40)). Using [**P**] and $\overline{\phi}_i$, the deformation of the spring in each mode ($\overline{\psi}_i$) is obtained from equation (41). Knowing α_i's from equation (43) and using equation (52), the coefficients of the frequency–amplitude equation (68) are obtained. The final expressions of the frequency–amplitude relationships for the first three modes corresponding to the two spring models, are:

6.3.1. *Fifth order spring model*

$$\omega_{N1} = 1{\cdot}138 - 20{\cdot}1568\hat{A}^2 - 1{\cdot}487626454 \times 10^2\hat{A}^4 + 3{\cdot}188617261 \times 10^4\hat{A}^4,$$

$$\omega_{N2} = 3{\cdot}408 - 3{\cdot}947019815 \times 10^{-2}\hat{A}^2 - 1{\cdot}904996008 \times 10^{-4}\hat{A}^4 + 4{\cdot}780973363\hat{A}^4,$$

$$\omega_{N3} = 7{\cdot}924 - 8{\cdot}797674851 \times 10^4\hat{A}^2 - 4{\cdot}070122676 \times 10^8\hat{A}^4 + 2{\cdot}426085485 \times 10^{10}\hat{A}^4.$$

6.3.2. *Seventh order spring model*

$$\omega_{N1} = 1{\cdot}138 - 2{\cdot}793\hat{A}^2 - 2{\cdot}8553 \times 10^2\hat{A}^4 + 8{\cdot}657906 \times 10^4\hat{A}^4 + 1{\cdot}41639283 \times 10^6\hat{A}^6 - 4{\cdot}32084 \times 10^3\hat{A}^6 - 9{\cdot}50547154 \times 10^7\hat{A}^6,$$

$$\omega_{N2} = 3{\cdot}408 - 6{\cdot}7618 \times 10^{-2}\hat{A}^2 - 5{\cdot}5908 \times 10^{-5}\hat{A}^4 + 17{\cdot}8501\hat{A}^4 + 2{\cdot}36143 \times 10^{-1}\hat{A}^6 - 6{\cdot}8414 \times 10^{-7}\hat{A}^6 - 1{\cdot}66869 \times 10^{3}\hat{A}^6,$$

$$\omega_{N3} = 7{\cdot}930 - 1{\cdot}226218 \times 10^{5}\hat{A}^2 - 7{\cdot}900145\hat{A}^4 + 6{\cdot}650156\hat{A}^4 + 6{\cdot}855182 \times 10^{14}\hat{A}^6 - 7{\cdot}532292 \times 10^{13}\hat{A}^6 - 1{\cdot}277168 \times 10^{16}\hat{A}^6.$$

The variations of the first three natural frequencies with amplitude of oscillation are shown in Figures 7–9. From Figure 7, it can be seen that with the seventh order approximation, the first natural frequency decreases continuously with the amplitude, whereas with the fifth order approximation, the frequency initially decreases up to an amplitude of 0·018 and then shows an increase with a further amplitude increase. The reason for this behaviour can be attributed to the stiffening nature of the fifth order approximation of the spring at high amplitudes, as shown in Figure 3. Similar behaviour is depicted by the third natural frequency as can be seen from Figure 9. However, as in the case of a linear spring, for the particular points of attachment (of the spring) considered here, the second natural frequency is least affected by the spring and hence by its non-linearity (Figure 8).

Figure 10 shows the nature of variation of the non-linear first natural frequency with amplitude as one uses different orders of approximation. The range of validity (over the amplitude levels) of different orders of approximation is obvious from the figure.

7. CONCLUSIONS

An idealised model for a bearingless rotor blade has been presented for the purpose of dynamic analysis. The highly non-linear viscoelastic characteristics of the elastomeric damper is modelled by a parallel combination of spring and damper elements. The stiffness and damping parameters of the model are identified from a set of experimental data taken from the literature. The stiffness element can be approximated by two polynomial functions having fifth or seventh order expansions depending on the desired range of validity. The alternate polynomial coefficients are found to be of opposite signs.

Both linear and non-linear free vibration of the rotating blade under flap bending have been studied. For the linear problem, two different solution techniques, one based on power series expansion and the other based on Rayleigh–Ritz principle, were used. Natural frequencies obtained from these two methods are found to be in excellent agreement. For the range of parameters used in this study which are close to practical situations, it was observed that the effect of elastomeric spring has a relatively high influence on the third mode; a moderate influence on the first mode and less influence on the second mode. In the non-linear analysis, a numerical–perturbation technique is applied to determine the frequency–amplitude relationship. It is concluded that up to a fairly high value of amplitude, not normally to be exceeded in practice, a seventh order expansion is sufficient to correctly predict the frequency–amplitude relationship. If the amplitude level is lower, one can use an expression up to the fifth order and still get accurate results while saving on the computational effort. The alternating signs in the polynomial, expressing the restoring force, prevents the non-linear

characteristic to be monotonically softening or hardening. Consequently, the non-linear natural frequency is somewhat insensitive to the value of the amplitude of oscillation.

REFERENCES

1. H. Huber 1992 *Eighteenth European Rotorcraft Forum*, Avignon, France. Will rotor hubs lose their bearings? A survey of bearingless main rotor development.
2. J. L. Potter *Lord Library No. LL*2120. Improving reliability and eliminating maintenance with elastomeric dampers for rotor systems.
3. D. P. McGuire *Lord Library No. LL*2133. The application of elastomeric lead–lag dampers to helicopter rotors.
4. W. G. Bousman, R. A. Ormiston and P. H. Mirick 1983 39*th Annual Forum of the American Helicopter Society*, St. Louis, USA. Design considerations for bearingless rotor hubs.
5. D. H. Hodges and E. H. Dowell 1974 *NASA TN D*-7818. Non-linear equations of motion for the elastic bending and torsion of twisted non-uniform rotor blades.
6. A. Rosen and P. P. Friedmann 1979 *Journal of Applied Mechanics* **46**, 161–168. The non-linear behavior of elastic slender straight beams undergoing small strains and moderate rotations.
7. K. R. Kaza and R. G. Kvaternik 1977 *NASA TM*-74059. Non-linear aeroelastic equations for combined flapwise bending, chordwise bending, torsion and extension of twisted non-uniform rotor blades in forward flight.
8. O. A. Bauchau 1985 *Journal of Applied Mechanics* **52**, 416–422. A beam theory for anisotropic materials.
9. E. H. Dowell, J. Traybar and D. H. Hodges 1977 *Journal of Sound and Vibration* **50**, 533–544. An experimental theoretical correlation study of non-linear bending and torsion deformations of a cantilever beam.
10. D. H. Hodges 1978 *AIAA Journal* **17**, 400–407. A theoretical technique for analyzing aeroelastic stability of bearingless rotors.
11. D. H. Hodges 1979 *Journal of the American Helicopter Society* **24**, 2–9. An aeromechanical stability analysis for bearingless rotor helicopters.
12. N. T. Sivaneri and I. Chopra 1984 *Journal of the American Helicopter Society* **29**, 42–51. Finite element analysis for bearingless rotor blade aeroelasticity.
13. A. L. Dull and I. Chopra 1988 *Journal of the American Helicopter Society* **33**, 38–46. Aeroelastic stability of bearingless rotors in forward flight.
14. J. Jang and I. Chopra 1988 *Journal of the American Helicopter Society* **33**, 20–29. Ground and air resonance of an advanced bearingless rotor in hover.
15. F. Gandhi and I. Chopra 1994 *American Helicopter Society Aeromechanical Specialists Conference*, San Francisco, USA. An analytical model for a non-linear elastomeric lag damper and its effect on aeromechanical stability in hover.
16. G. Housmann 1986 *Twelfth European Rotorcraft Forum*, Garmisch-Partenkirchen, Germany, No. 70. Structural analysis and design considerations of elastomeric dampers with viscoelastic material behavior.
17. F. Felker, B. Lau, S. McLaughlin and W. Johnson 1987 *Journal of the American Helicopter Society* **34**, 45–53. Non-linear behavior of an elastomeric lag damper undergoing dual-frequency motion and its effect on rotor dynamics.
18. E. C. Smith, M. R. Beale, K. Govindswamy, M. J. Vascsinec and G. A. Lesieutre 1995 *American Helicopter Society* 51*st Annual Forum*, Fort Worth, USA. Formulation and validation of a finite element model for elastomeric lag dampers.
19. F. Gandhi, I. Chopra and S. W. Lee 1994 (*SPIE*) *North American Conference on Smart Structures and Materials*, Orlando, USA. A non-linear viscoelastic damper model: constitutive equation and solution scheme.

20. G. L. Anderson 1975 *International Journal for Non-linear Mechanics* **10**, 223–236. On the extensional and flexural vibrations of rotating bars.
21. P. Minguet and J. Dugundji 1990 *AIAA Journal* **28**, 1580–1588. Experiments and analysis for composite blades under large deflection: part 2—dynamic behavior.
22. A. H. Nayfeh, D. T. Mook and D. W. Lobitz 1974 *AIAA Journal* **12**, 1222–1228. Numerical–perturbation method for the non-linear analysis of structural vibrations.
23. M. Pakdemirli and A. H. Nayfeh 1994 *Journal of Vibration and Acoustics* **116**, 433–439. Non-linear vibration of a beam-spring-mass system.
24. A. H. Nayfeh and S. A. Nayfeh 1994 *Journal of Vibration and Acoustics* **117**, 199–205. Non-linear normal modes of a continuous system with quadratic nonlinearities.
25. A. H. Nayfeh, C. Chin and S. A. Nayfeh 1995 *Journal of Vibration and Acoustics* **117**, 477–481. Non-linear normal modes of a cantilever beam.
26. A. H. Nayfeh 1996 *Differential equation and chaos* (N. H. Ibragimov editor). Johannesburg: New Age International (P).
27. J. K. Suresh, C. Venkatesan and V. Ramamurti 1990 *Journal of Sound and Vibration* **143**, 503–519. Structural dynamic analysis of composite beams.
28. P. Friedmann, K. Yuan, T. Millott and C. Venkatesan 1994 *AIAA Dynamics Specialists Conference*, Hilton Head, USA. *AIAA* 94-1722. Correlation studies for hingeless rotors in forward flight.
29. P. K. Gupta, C. Venkatesan and O. Singh 1997 *Proceedings of* 48*th AGM*, *Aeronautical Society of India*. Structural dynamics of rotor blades with precone–presweep–predroop–pretwist and torque offset including hub motion.